



Research article

On the effective method for the space-fractional advection-diffusion equation by the Galerkin method

Haifa Bin Jebreen^{1,*} and Hongzhou Wang²

¹ Department of mathematics, College of Science, King Saud University, P.O. Box 2455, Riyadh 11451, Saudi Arabia

² Beijing Key Lab on Mathematical Characterization, Analysis, and Applications of Complex Information, MIIT Key Laboratory of Mathematical Theory and Computation in Information Security, School of Mathematics and Statistics, Beijing Institute of Technology, Beijing 100081, China

* **Correspondence:** Email: hjebreen@ksu.edu.sa.

Abstract: The present work is dedicated to a study that focuses on solving space-fractional advection-diffusion equations (SFADEs) using the Galerkin method. Through our analysis, we demonstrate the effectiveness of this approach in solving the considered equations. After introducing the Chebyshev cardinal functions (CCFs), the Caputo fractional derivative (CFD) was represented based on these bases as an operational matrix. Applying the Galerkin method reduces the desired equation to a system of algebraic equations. We have proved that the method converges analytically. By solving some numerical examples, we have demonstrated that the proposed method is effective and yields superior outcomes compared to existing methods for addressing this problem.

Keywords: Chebyshev cardinal functions; space-fractional advection-diffusion equations; Galerkin method; convergence analysis

Mathematics Subject Classification: 26A33, 54A25, 65M70

1. Introduction

As we know, fractional calculus is a mathematical topic whose use dates back to recent years. It has been discovered that fractional derivatives of various types [1] can be used to model many systems across multiple fields, including viscoelastic materials, electromagnetic fields, control systems, electrochemical reactions, porous media flow, and more [2–5]. Various analytical and numerical techniques have been developed and implemented to investigate and solve fractional differential equations, such as the wavelet method [6–9], Adomian decomposition [10], the Kuratowski measure of

noncompactness technique [11], the B-spline collocation method [12], the least-squares finite element method [13], the adaptive-grid technique [14], multi-step methods [15], an implicit integration factor method [16], the Petrov-Galerkin finite element-meshfree [17], fast second-order accurate difference schemes [18], etc.

This paper primarily focuses on solving a special form of FPDEs (fractional partial differential equations) through the Galerkin method. The equation is represented as

$$\begin{cases} v_t + uv_x + w \frac{\partial^\mu v}{\partial x^\mu} + pv = f, & x \in [a, b], \quad t \in (0, T), \\ v|_{t=0} = g(x), & x \in [a, b], \\ v|_{x=a} = h_a(t), \quad v|_{x=b} = h_b(t), & t \in (0, T), \end{cases} \quad (1.1)$$

where $\mu \in (1, 2]$, v_x is the advection item, the anomalous diffusion $\frac{\partial^\mu v}{\partial x^\mu}$ is the Caputo fractional derivative (CFD) with respect to variable x , the functions u, w, p belong to space $C([a, b] \times (0, T))$, $g(x) \in C[a, b]$, and $h_a, h_b \in C(0, T)$. The existence and uniqueness of the solution of Eq (1.1) are investigated in detail in [19].

Equation (1.1) can refer to different PDEs (partial differential equations) based on the values of μ and f . We have classical PDEs if $\mu \in \mathbb{Z}^+$. In the case where $\mu = 2$ and $f = 0$, it usually denotes the standard Fokker-Planck equation. This equation is commonly used to describe the Brownian motion of particles. If μ is equal to 2 and $p \in \mathbb{R}$, then it represents the classical form of the advection dispersion equation. However, if μ is not an integer, it is associated with the phenomenon of anomalous diffusion. In anomalous diffusion, superdiffusion can be characterized by the space fractional derivative of order $\mu \in (1, 2]$. The anomalous diffusion involves the non-linear increase of the mean squared displacement over time in a power-law form $\langle x^2(t) \rangle = k_\mu t^\mu$, where k_μ is the diffusion coefficient, and the superdiffusion corresponds to $\mu \in (1, 2)$ being exactly the order of the space fractional derivative [20,21]. On the other hand, the space fractional advection-diffusion equation is an effective tool to describe superdiffusion with advection motion. For more details, we refer the reader to [21].

The advection-diffusion equation with space fractional derivative (1.1) appears naturally in many practical problems. It can be used to model the probability distribution of particles exhibiting advection and superdiffusion, such as nonlocal and non-Fickian flows in porous media [22]. Some numerical schemes have been developed and implemented to solve the space-fractional advection-diffusion equation. Zheng et al. [23] used a finite element method to solve Eq (1.1). They investigated the error estimate and presented two numerical examples to confirm their theoretical analysis. In [20], the authors have used the spectral collocation method to solve SFADEs numerically. The finite volume method has been used for solving (1.1) where stability and convergence of the scheme are investigated in [24]. Jannelli et al. [25] utilized a new technique to solve Eq (1.1). They first transformed this equation into fractional ordinary differential equations through the fractional Lie symmetries. They then used an implicit trapezoidal method to solve the resulting ODE. In [26,27], the authors have used a semi-discretization method that applies the weighted essentially non-oscillatory scheme and implicit integration factor method for space and time discretization, respectively. Our main goal is to introduce and implement a practical, efficient, and simple numerical method to reduce the computational cost while solving these types of equations.

Cardinal functions have a unique property of having non-zero values at only one point. This makes it easy to approximate any function and avoid any integration to find the coefficients in the corresponding

expansion. The method for constructing these types of functions can be found in reference [28]. It provides a general framework for building these functions. These functions are widely used to solve equations because of their high approximation power and unique characteristics. In [12], the authors studied the collocation method based on Chebyshev cardinal functions (CCFs) to solve special PDEs. These bases are used to solve the fractional Sturm-Liouville equation [29,30]. A pseudospectral method based on the CCFs has been applied for solving fractional integro-differential equations [31]. Shahriari et al. [32] studied the Dirac operator using the pseudospectral method based on CCFs.

The subsequent sections of the paper are structured in the following manner: Chebyshev cardinal polynomials and their properties are reviewed and introduced in Section 2. The Galerkin method is applied to solve SFADEs (1.1), in Section 3. Section 4 is devoted to demonstrating the practicality and precision of the method. Section 5 of our paper provides a concise summary of our findings.

2. Chebyshev cardinal polynomials

Before introducing the Chebyshev cardinal functions (CCFs), we must review the Chebyshev polynomials and some related concepts critical for the CCFs' introduction. Recall that the TChebyshev polynomials (Chebyshev polynomials of the first kind) with degree J on $[-1, 1]$ are specified through

$$T_J(\cos(\theta)) = \cos(J\theta), \quad J = 0, 1, \dots,$$

and their roots are given by

$$r_j := \cos\left(\frac{(j + 1/2)\pi}{J}\right), \quad \forall j = 0, 1, \dots, J - 1. \quad (2.1)$$

To shift the Chebyshev polynomials for generic intervals $[a, b]$, the shifted Chebyshev polynomials T_J^* can be specified through a simple change of variable, viz.,

$$T_J^*(t) := T_J\left(\frac{2(t - a)}{b - a} - 1\right). \quad (2.2)$$

Considering the aforementioned change of variable, it is easy to obtain the roots of T_J^* by

$$t_j = \frac{(r_j + 1)(b - a)}{2} + a, \quad j = 0, 1, \dots, J - 1. \quad (2.3)$$

According to the ability of CCFs in numerical simulations, as mentioned for a few of them in the Introduction section, we shall introduce these functions. One of the notable cardinal functions is the cardinal function obtained through orthogonal functions. Considering the properties of Chebyshev polynomials, it can be said that CCFs are among the most important orthogonal cardinal functions [28]. Considering $T_{J+1,t}^*(t_j)$ as the derivative of function $T_{J+1}^*(t)$ with respect to the variable t , Chebyshev cardinal functions can be specified by

$$C_j(t) = \frac{T_{J+1}^*(t)}{T_{J+1,t}^*(t_j)(t - t_j)}, \quad j = 0, 1, \dots, J. \quad (2.4)$$

Cardinality is an impressive feature of these polynomials, which means

$$C_j(t_i) = \delta_{ji}, \quad (2.5)$$

in which δ_{ji} indicates the Kronecker delta. This property is mostly important as it enables us to approximate any function $w \in \mathcal{H}^\alpha([a, b])$ (the Sobolev space $\mathcal{H}^\alpha([a, b])$ will be briefly introduced) easily and without integration in finding the coefficients, viz.,

$$v(t) \approx \sum_{j=1}^{J+1} v(t_j) C_j(t) := v_{J+1}(t). \quad (2.6)$$

In what follows, we will provide a brief definition of Sobolev space and its norm, since it will be necessary for our purposes. The Sobolev space, usually denoted by $\mathcal{H}^n([a, b])$, encompasses functions $v(t)$ such that they have continuous derivatives of order up to $n \in \mathbb{N}$, subject to the condition $\mathcal{D}^\mu v \in L^2([a, b])$ (\mathcal{D} indicates the derivative operator):

$$\mathcal{H}^n([a, b]) = \left\{ v \in C^n([a, b]) : \mathcal{D}^\mu v \in L^2([a, b]), \mathbb{N} \ni \mu \leq n \right\},$$

with the norm

$$\|v\|_{\mathcal{H}^n([a, b])}^2 = \sum_{j=0}^n \|v^{(j)}(t)\|_{L^2([a, b])}^2, \quad (2.7)$$

and the semi-norm

$$|v|_{\mathcal{H}^{n, J}([a, b])}^2 = \sum_{j=\min\{n, J\}}^J \|v^{(j)}(t)\|_{L^2([a, b])}^2. \quad (2.8)$$

Lemma 2.1. *Let $J \geq 0$. The error of approximation (2.5), obtained using the shifted Chebyshev nodes $\{t_j\}_{j=1}^J$, can be bounded:*

$$\|v - v_J\|_{L^2([a, b])} \leq C J^{-n} |v|_{\mathcal{H}^{n, J}([a, b])}, \quad (2.9)$$

where the constant C is independent of J . Furthermore, it can be verified that

$$\|v - v_J\|_{\mathcal{H}^l([a, b])} \leq C J^{2l-1/2-n} |v|_{\mathcal{H}^{n, J}([a, b])}, \quad n \geq 1, 1 \leq l \leq n. \quad (2.10)$$

2.1. Operational matrix of derivative

To specify the operational matrix of the derivative for CCFs, we must first take the derivative of these functions. Then, we approximate the results obtained from the derivation based on CCFs. We denote this matrix by D , which satisfies

$$\mathcal{D}(C)(t) = DC(t). \quad (2.11)$$

To determine the elements of D , it is necessary to follow a specific process that involves using the approximation (2.6). By adhering to this methodology, one can evaluate the various elements of D with high accuracy, i.e.,

$$D_{j,i} = \mathcal{D}(C_j)(t_i). \quad (2.12)$$

It is worth noting that there is an alternative formula to present CCFs [29, 30]:

$$C_j(t) = \delta_j \prod_{\nu=1, \nu \neq j}^{J+1} (t - t_\nu), \quad (2.13)$$

where $\delta_j = 2^{2^{J+1}} / ((b-a)^{J+1} T_{J+1,t}^*(t_j))$. Upon applying operator \mathcal{D} on both sides of (2.13) and taking into account (2.4), we get

$$\begin{aligned} \mathcal{D}(C_j)(t) &= \delta_j \prod_{\substack{v=1 \\ v \neq j}}^{J+1} \mathcal{D}(t-t_v) = \delta_j \sum_{\substack{k=1 \\ k \neq j}}^{J+1} \prod_{\substack{v=1 \\ v \neq j,k}}^{J+1} (t-t_v) \\ &= \sum_{\substack{k=1 \\ k \neq j}}^{J+1} \frac{T_{J+1}^*(t)}{(t-t_j)(t-t_k)T_{J+1,t}^*(t_j)} \\ &= \sum_{\substack{k=1 \\ k \neq j}}^{J+1} \frac{1}{(t-t_k)} C_j(t). \end{aligned} \quad (2.14)$$

Now, it follows from (2.12) and (2.14) that

$$D_{j,i} = \mathcal{D}(C_j)(t_i) = \begin{cases} \sum_{\substack{k=1 \\ k \neq j}}^{J+1} \frac{1}{(t_i-t_k)}, & j = i, \\ \delta_j \prod_{\substack{v=1 \\ v \neq j,i}}^{J+1} (t_i-t_v), & j \neq i. \end{cases}$$

2.2. Operational matrix of fractional integration

It is worth noting that fractional integrals are a generalization of the classical integrals, and they play a vital role in many areas of research, including signal processing, fluid mechanics, and statistical physics. The fractional integrals are defined as

$$\mathcal{J}_0^\mu(v)(t) := \frac{1}{\Gamma(\mu)} \int_0^t (t-\theta)^{\mu-1} w(\theta) d\theta, \quad t \in [0, 1], \quad \mu \in \mathbb{R}^+, \quad (2.15)$$

where $\Gamma(\mu)$ denotes the gamma function.

Similar to the operational matrix for the derivative, we note that a square matrix I_μ exists to represent the operation of the fractional integral operator on CCFs, i.e.,

$$\mathcal{J}_0^\mu(C(t)) \approx I_\mu C(t), \quad t \in (0, 1). \quad (2.16)$$

Demonstrating that the elements of this matrix can be obtained through the use of (2.6) is straightforward. Strictly speaking, we can evaluate the elements of I_μ as follows:

$$(I_\mu)_{j,i} = \mathcal{J}_0^\mu(C_j(t_i)). \quad (2.17)$$

Based on the calculations presented in [33], it can be inferred that

$$\prod_{\substack{v=1 \\ v \neq j}}^{J+1} (t-t_v) = \sum_{v=0}^J \kappa_{j,v} t^{J-v}, \quad (2.18)$$

in which

$$\kappa_{j,0} = 1, \kappa_{j,\nu} = \frac{1}{\nu} \sum_{k=0}^{\nu} \varrho_{j,k} \kappa_{j,\nu-k}, \quad j = 1, \dots, J+1, \nu = 1, \dots, J,$$

and

$$\varrho_{j,k} = \sum_{\substack{i=1 \\ i \neq j}}^{J+1} t_i^k, \quad j = 1, \dots, J+1, k = 1, \dots, J.$$

Taking into account (2.13), the CCFs may be stated by

$$C_j(t) = \delta_j \sum_{\nu=0}^J \kappa_{j,\nu} t^{J-\nu}. \quad (2.19)$$

Considering (2.19), Eq (2.17) leads to

$$\begin{aligned} \mathcal{J}_0^\mu(C_j(t)) &= \delta_j \mathcal{J}_0^\mu \left(\sum_{\nu=0}^J \kappa_{j,\nu} t^{J-\nu} \right) \\ &= \delta_j \sum_{\nu=0}^J \kappa_{j,\nu} \mathcal{J}_0^\mu(t^{J-\nu}) \\ &= \delta_j \sum_{\nu=0}^J \kappa_{j,\nu} \frac{\Gamma(J-\nu+1)}{\Gamma(J-\nu+\mu+1)} t^{J-\nu+\mu}. \end{aligned}$$

Thus, the entries of I_μ can be evaluated exactly as

$$(I_\mu)_{j,i} = \delta_j \sum_{\nu=0}^J \kappa_{j,\nu} \frac{\Gamma(J-\nu+1)}{\Gamma(J-\nu+\mu+1)} t_i^{J-\nu+\mu}. \quad (2.20)$$

2.3. Operational matrix of fractional derivative

To obtain the operational matrix for the fractional derivative in the Caputo sense, we adopt a method that circumvents the need to determine its elements directly. This approach will consider the relation between the CFD and the fractional integral operator. To this end, let us start with the definition of the CFD.

Definition 2.1. [34] Let $\mu \in \mathbb{R}^+$ and $m := \lceil \mu \rceil \in \mathbb{N}$ ($\lceil \cdot \rceil$ denotes the ceiling function). The CFD is denoted by

$${}^c \mathcal{D}_0^\mu(v)(t) := \frac{1}{\Gamma(m-\mu)} \int_0^t \frac{f^{(m)}(\theta) d\theta}{(t-\theta)^{\mu-m+1}} =: \mathcal{J}_0^{m-\mu} \mathcal{D}^m(v)(t), \quad (2.21)$$

where $\mathcal{D}^m := \frac{d^m}{dt^m}$.

Lemma 2.2. [34] Let $\mu \in \mathbb{R}^+$. Then, we have

$$\|\mathcal{J}_0^\mu(v)\|_q \leq \frac{1}{\Gamma(\mu+1)} \|v\|_q, \quad 1 \leq q \leq \infty. \quad (2.22)$$

Considering (2.21) and using Lemma 2.2, we can conclude that

$$\|\mathcal{J}_0^{m-\mu} \mathcal{D}^m(v)\|_q \leq \frac{1}{\Gamma(m-\mu+1)} \|\mathcal{D}^m(v)\|_q. \quad (2.23)$$

Considering the definition 2.1, we can replace the fractional derivative operator ${}^c \mathcal{D}_0^\mu$ with $\mathcal{J}_0^{m-\mu} \mathcal{D}^m$. This helps us specify the CFD operational matrix using the operational matrices D and I_μ , viz.,

$${}^c \mathcal{D}_0^\mu(C)(t) = \mathcal{J}_0^{m-\mu} \mathcal{D}^m(C(t)) \approx D^m(I_{m-\mu})C(t). \quad (2.24)$$

Thus, the CFD operational matrix is determined by

$$D_\mu = D^m(I_{m-\mu}). \quad (2.25)$$

3. Materials and methods

The present section will concentrate on solving the space fractional advection-diffusion equation (FADE) by employing an efficient and precise approach based on the Galerkin method.

Considering the space of all polynomials up to degree $J+1$ with $\Pi_{J+1}(t)$, the projection operator \mathcal{P} is utilized for mapping any continuous functions onto $\Pi_{J+1}(t)$. Given (2.6), we have

$$v(t) \approx \mathcal{P}(v)(t) = V^T C(t) := v_{J+1}. \quad (3.1)$$

To implement the Galerkin algorithm, the unknown solution $v(x, t)$ should be projected to the two-dimensional polynomial space $\Pi_{J+1}(x, t)$,

$$v(x, t) \approx \mathcal{P}(v)(x, t) = \sum_{i=1}^{J+1} \sum_{j=1}^{J+1} v_{i,j} C_i(x) C_j(t) = C^T(x) V C(t) = v_{J+1}(x, t), \quad (3.2)$$

in which $V \in \mathbb{R}^{(J+1) \times (J+1)}$ consists of unknown elements. Substituting v_{J+1} instead of v in (1.1) leads to

$$v_{J+1,t} + uv_{J+1,x} + w \frac{\partial^\mu v_{J+1}}{\partial x^\mu} + pv_{J+1} \approx f, \quad x \in [a, b], \quad t \in (0, T]. \quad (3.3)$$

Now, it is straightforward to obtain the following approximations for all terms in (3.3).

- Considering the operational matrix for the derivative and using (3.2), we get

$$v_{J+1,t} \approx \mathcal{P}(v_{J+1,t})(x, t) = C^T(x) V D C(t). \quad (3.4)$$

- The first step to approximate the second term is obtained using the operational matrix for the derivative and Eq (3.2), as follows:

$$v_{J+1,x} \approx \mathcal{P}(v_{J+1,x})(x, t) = C^T(x) D^T V C(t). \quad (3.5)$$

We multiply the functions $v_{J+1,x}$ and u together to get the function $g_1(x, t) := uv_{J+1,x}$. Then, the function g_1 can be approximated by the projection operator \mathcal{P} , i.e.,

$$g_1(x, t) \approx \mathcal{P}(g_1)(x, t) = C^T(x) G_1 C(t), \quad (3.6)$$

where $G_1 \in \mathbb{R}^{(J+1) \times (J+1)}$, whose elements depend on the unknowns V . In other words, each element of G_1 is a linear equation of unknowns $v_{i,j}$, $i, j = 1, \dots, J+1$.

- Similar to the second item, we estimate $\frac{\partial^\mu v_{J+1}}{\partial x^\mu}$ using the CFD operational matrix D_μ as

$$\frac{\partial^\mu v_{J+1}}{\partial x^\mu} \approx C^T(x) D_\mu^T V C(t). \quad (3.7)$$

Putting $g_2 := w \frac{\partial^\mu v_{J+1}}{\partial x^\mu}$ and approximating it using the projection operator \mathcal{P} , we have

$$g_2(x, t) \approx \mathcal{P}(g_2)(x, t) = C^T(x) G_2 C(t), \quad (3.8)$$

where each element of $G_2 \in \mathbb{R}^{(J+1) \times (J+1)}$ is a linear equation of unknowns $v_{i,j}$, $i, j = 1, \dots, J+1$.

- For the fourth item, similar to the two previous items, we can write

$$g_3(x, t) \approx \mathcal{P}(g_3)(x, t) = C^T(x) G_3 C(t), \quad (3.9)$$

in which $g_3 := p v_{J+1}$ and $G_3 \in \mathbb{R}^{(J+1) \times (J+1)}$. It is easy to show that these matrix elements depend on unknowns V .

- The function f on the right hand side is easily approximated as follows:

$$f(x, t) \approx \mathcal{P}(f)(x, t) = C^T(x) F C(t) = f_{J+1}(x, t), \quad (3.10)$$

where $F \in \mathbb{R}^{(J+1) \times (J+1)}$.

Now, we substitute Eqs (3.4), (3.6), (3.8), (3.9), and (3.10) into (3.3) to introduce the residual function

$$r_{J+1}(x, t) := C^T(x) (VD + G_1 + G_2 + G_3 - F) C(t). \quad (3.11)$$

To implement the Galerkin scheme, r_{J+1} must satisfy $\langle r_{J+1}(x, t), C_i(x) C_j(t) \rangle = 0$, $i, j = 1, \dots, J$. This yields the system

$$VD + G_1 + G_2 + G_3 = F. \quad (3.12)$$

This system is linear, and we can write it as

$$G\bar{V} = \bar{F}, \quad (3.13)$$

where the matrices V and F are converted into the vectors \bar{V} and \bar{F} , respectively, by the matrix-to-vector conversion by row, and the matrix $G \in \mathbb{R}^{(J+1)^2 \times (J+1)^2}$ can be obtained by extracting the coefficients of the linear system (3.12) using the Maple command $G[i, j] := \text{Coeff}(\bar{H}_i, \bar{V}_j)$ (where \bar{H} is the matrix-to-vector conversion by row of $H := VD + G_1 + G_2 + G_3$). Solving this system by the GMRES method (generalized minimal residual method) [35] leads to the unknown solution $v(x, t)$.

3.1. Convergence analysis

Motivated by [36, 37], for the function $v(x, t) \in C^{2J}[a, b]^2$, we can bound the error of approximation as follows.

$$|v(x, t) - v_J(x, t)| \leq M_v \left(\frac{1}{2} \right)^J \frac{1}{2^{J-1} J!} \left(2 + \left(\frac{1}{2} \right)^J \frac{1}{2^{J-1} J!} \right), \quad (3.14)$$

in which $v_J = \mathcal{P}(v)$, and

$$M_v = \max \left\{ \sup_{\xi \in [0,1]} \left| \frac{\partial^J}{\partial x^J} v(\xi, t) \right|, \sup_{\tau \in [0,1]} \left| \frac{\partial^J}{\partial t^J} v(x, \tau) \right|, \sup_{\xi', \tau' \in [0,1]} \left| \frac{\partial^{2J}}{\partial x^J \partial t^J} v(\xi', \tau') \right| \right\}.$$

In a more abstract form, the residual (3.11) and the residual for Eq (1.1) can be written as

$$r_{J+1}(x, t) := \mathcal{P} \left(v_{J+1,t} + uv_{J+1,x} + w \frac{\partial^\mu v_{J+1}}{\partial x^\mu} + pv_{J+1} - f \right), \quad (3.15)$$

$$r(x, t) := v_t + uv_x + w \frac{\partial^\mu v}{\partial x^\mu} + pv - f, \quad (3.16)$$

respectively. Subtracting (3.16) from (3.15) gives

$$R(x, t) := v_t + uv_x + w \frac{\partial^\mu v}{\partial x^\mu} + pv - f - \mathcal{P} \left(v_{J+1,t} + uv_{J+1,x} + w \frac{\partial^\mu v_{J+1}}{\partial x^\mu} + pv_{J+1} - f \right). \quad (3.17)$$

Taking the L^2 -norm from both sides of (3.17), leads to

$$\begin{aligned} \|R\| &\leq \|v_t - \mathcal{P}(v_{J+1,t})\| + \|uv_x - \mathcal{P}(uv_{J+1,x})\| + \|w \frac{\partial^\mu v}{\partial x^\mu} - \mathcal{P}(w \frac{\partial^\mu v_{J+1}}{\partial x^\mu})\| \\ &\quad + \|pv - \mathcal{P}(pv_{J+1})\| + \|f - \mathcal{P}(f)\|. \end{aligned} \quad (3.18)$$

Taking into account Eqs (2.24) and (3.14), we obtain

•

$$\begin{aligned} \|v_t - \mathcal{P}(v_{J+1,t})\| &\leq \|v_t - v_{J+1,t}\| + \|v_{J+1,t} - \mathcal{P}(v_{J+1,t})\| \\ &\leq C_1 \left(\frac{1}{2} \right)^{J+1} \frac{1}{2^J (J+1)!} \left(2 + \left(\frac{1}{2} \right)^{J+1} \frac{1}{2^J (J+1)!} \right), \end{aligned} \quad (3.19)$$

where $C_1 := M_{v_t} + M_{v_{J+1,t}}$.

- As the function u is continuous, a constant c_u exists, such that for all (x, t) in the domain of u , the value of $u(x, t)$ satisfies $|u| \leq c_u$. Using this assumption, we have

$$\begin{aligned} \|uv_x - \mathcal{P}(uv_{J+1,x})\| &\leq \|uv_x - uv_{J+1,x}\| + \|uv_{J+1,x} - \mathcal{P}(uv_{J+1,x})\| \\ &\leq C_2 \left(\frac{1}{2} \right)^{J+1} \frac{1}{2^J (J+1)!} \left(2 + \left(\frac{1}{2} \right)^{J+1} \frac{1}{2^J (J+1)!} \right), \end{aligned} \quad (3.20)$$

where $C_2 := c_u M_{v_x} + M_{uv_{J+1,x}}$

- As the function w is continuous, a constant c_w exists, such that for all (x, t) in the domain of w , the value of $w(x, t)$ satisfies $|w| \leq c_w$. Thus, we obtain

$$\begin{aligned} \|w \frac{\partial^\mu v}{\partial x^\mu} - \mathcal{P}(w \frac{\partial^\mu v_{J+1}}{\partial x^\mu})\| &\leq \|w \frac{\partial^\mu v}{\partial x^\mu} - w \frac{\partial^\mu v_{J+1}}{\partial x^\mu}\| + \|w \frac{\partial^\mu v_{J+1}}{\partial x^\mu} - \mathcal{P}(w \frac{\partial^\mu v_{J+1}}{\partial x^\mu})\| \\ &\leq C_3 \left(\frac{1}{2} \right)^{J+1} \frac{1}{2^J (J+1)!} \left(2 + \left(\frac{1}{2} \right)^{J+1} \frac{1}{2^J (J+1)!} \right), \end{aligned} \quad (3.21)$$

where $C_3 := \frac{c_w}{\Gamma(m-\mu+1)} M_{\mathcal{D}^m(v)} + M_{\frac{\partial^\mu v_{J+1}}{\partial x^\mu}}$.

- Similar to the previous item, there is a constant c_p such that $|p| \leq c_p$. This inequality helps us to obtain

$$\begin{aligned} \|pv - \mathcal{P}(pv_{J+1})\| &\leq \|pv - pv_{J+1}\| + \|pv_{J+1} - \mathcal{P}(pv_{J+1})\| \\ &\leq C_4 \left(\frac{1}{2}\right)^{J+1} \frac{1}{2^J(J+1)!} \left(2 + \left(\frac{1}{2}\right)^{J+1} \frac{1}{2^J(J+1)!}\right), \end{aligned} \quad (3.22)$$

where $C_4 := c_p M_v + M_{pv_{J+1}}$.

- Finally, we have

$$\|f - \mathcal{P}(f)\| \leq C_5 \left(\frac{1}{2}\right)^{J+1} \frac{1}{2^J(J+1)!} \left(2 + \left(\frac{1}{2}\right)^{J+1} \frac{1}{2^J(J+1)!}\right), \quad (3.23)$$

where $C_5 := M_f$.

To proceed, by substituting (3.19)–(3.23) into (3.18), we can find

$$\|R\| \leq C \left(\frac{1}{2}\right)^{J+1} \frac{1}{2^J(J+1)!} \left(2 + \left(\frac{1}{2}\right)^{J+1} \frac{1}{2^J(J+1)!}\right), \quad (3.24)$$

in which $C := \sum_{i=1}^5 C_i$.

It is straightforward to show that the presented method converges,

$$\lim_{J \rightarrow \infty} \|R\| \rightarrow 0. \quad (3.25)$$

4. Numerical results

By providing some numerical simulations, we can showcase the effectiveness of the present method. These examples will demonstrate how the method can provide practical solutions to various problems. To provide an overview of method efficiency, tables, and figures report absolute error

$$e_J = v(x, t) - v_J(x, t),$$

and L^2 -error

$$L^2 - error = \left(\int_0^1 |v(t) - v_J(t)|^2 \right)^{1/2}.$$

All examples were performed using Maple and Matlab software (version 2022). To have higher precision, we increase precision beyond 50 digits.

Example 4.1. As the first example, we utilize the presented scheme for

$$\begin{cases} v_t - \frac{\partial^\mu v}{\partial x^\mu} + v = f, & \mu = 1.7, \quad x \in [0, 2], \quad t \in [0, 1], \\ v(x, 0) = x^2(2-x)^2, & x \in [0, 2], \\ v(0, t) = v(2, t) = 0, & t \in [0, 1], \end{cases}$$

where

$$f(x, t) := -\frac{8((\mu^2 - 7\mu + 12)x^{2-\mu} + (3\mu - 12)x^{3-\mu} + 3x^{4-\mu})e^{-t}}{\Gamma(5 - \mu)},$$

and motivated by [23], $v(x, t) = e^{-t} x^2(2 - x)^2$ is the exact solution.

To verify that the presented method converges, Table 1 reports the L^2 -error. As we can see, the error reduces with the increase of J . Table 2 is tabulated to compare the finite element method [23] and the presented scheme. Figure 1 (left) demonstrates the L^2 -error versus J . Also, the right one shows the L^2 -error at different times and different choices of J . Figure 2 is plotted to confirm that the method converges.

Table 1. The L^2 -error and CPU time for Example 4.1.

J	5	6	7	8	9	10
L^2 -error	1.039×10^{-04}	6.334×10^{-06}	5.603×10^{-07}	2.842×10^{-08}	1.836×10^{-09}	7.954×10^{-11}
Time	0.094	0.103	0.125	0.266	0.484	0.718

Table 2. The comparison between the presented scheme and the finite element method [23] for Example 4.1.

t	Proposed method		[23]	
	$J = 8$	$J = 10$	$h = 1/160$	$h = 1/320$
L^2 -error	1.836×10^{-09}	7.954×10^{-11}	3.137×10^{-06}	7.839×10^{-07}

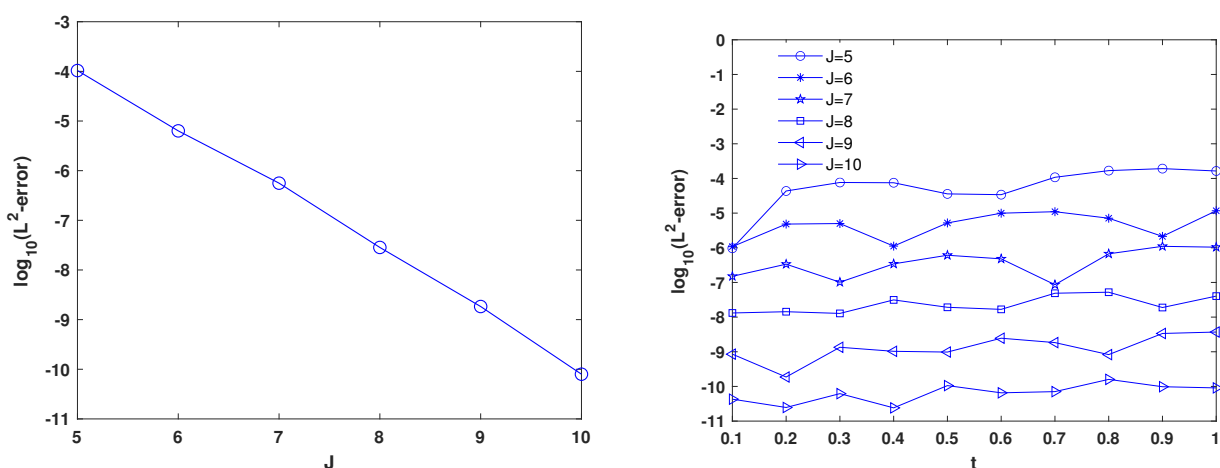


Figure 1. The L^2 -error obtained by different values of J (left) and the L^2 -error obtained by different values of J at different times (right) for Example 4.1.

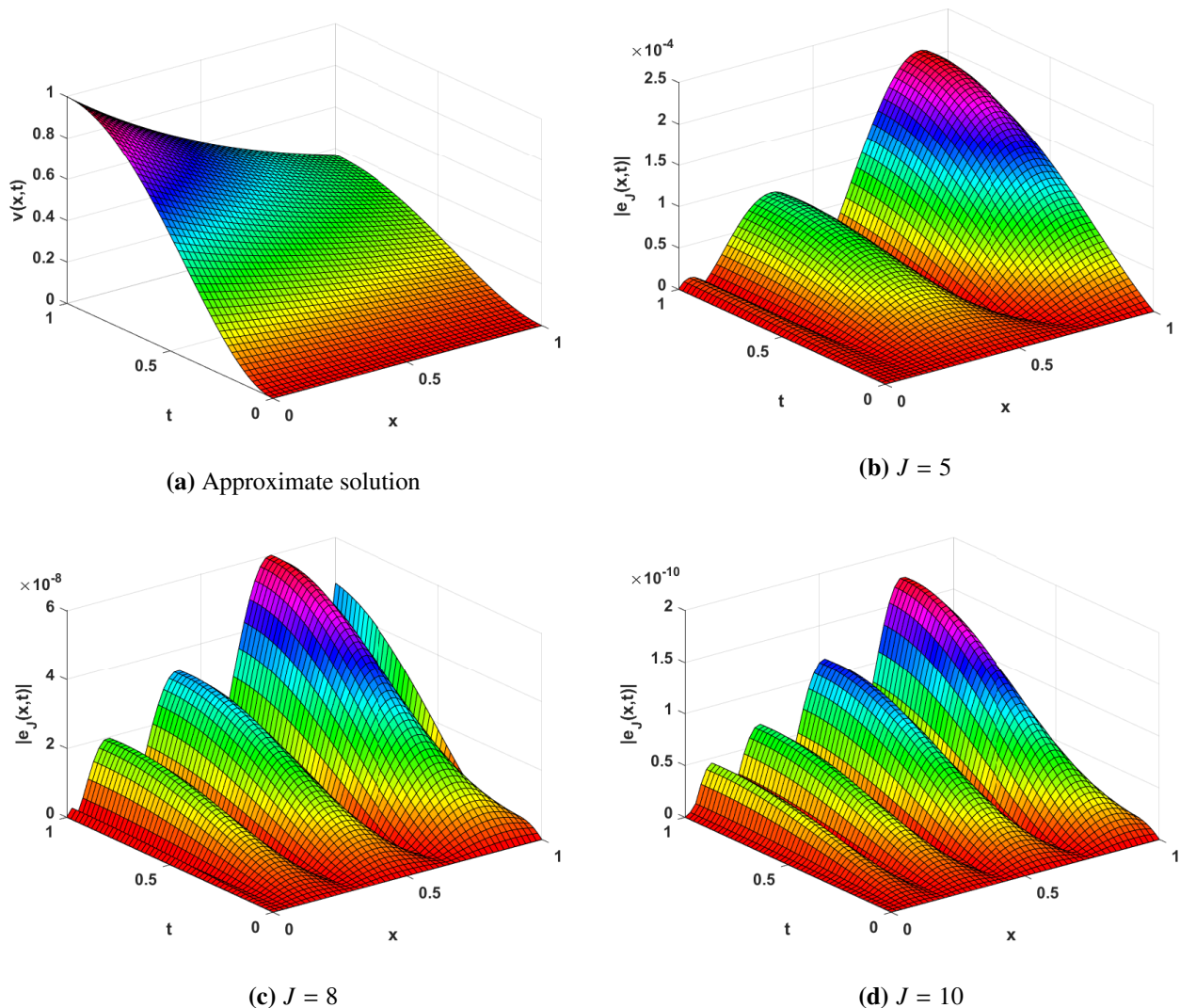


Figure 2. The plot of the approximate solution by choosing $J = 10$ and absolute error with different choices of J for Example 4.1.

Example 4.2. As with the first example, we utilize the presented scheme for

$$\begin{cases} v_t - \frac{1}{6}\Gamma(2.2)x^{2.8}\frac{\partial^{\mu}v}{\partial x^{\mu}} = -(1+x)e^{-t}x^3, & \mu = 1.8, \quad x \in [0, 2], \quad t \in [0, 1], \\ v(x, 0) = x^3, & x \in [0, 1], \\ v(0, t) = 0, \quad v(1, t) = e^{-t}, & t \in [0, 1]. \end{cases}$$

Motivated by [23], $v(x, t) = e^{-t}x^3$ is the exact solution.

We report the L^2 -error in Table 3. As we can see, the error reduces with the increase of J . Table 4 is tabulated to compare the finite element method [23] and the presented scheme. Figure 3 (left) demonstrates the L^2 -error versus J . Also, the right one shows the L^2 -error at different times and different choices of J . Figure 4 is plotted to confirm the method converges. To show the ability of the method to solve SFADE with a large time interval ($t \in [0, 10]$), Table 5 is tabulated. We must consider more bases for time to solve these types of examples. Due to the high density of Chebyshev polynomial

roots at the beginning and end of the interval, appropriate accuracy can be obtained. However, the error at the end of the interval will be slightly more than at the beginning. For more details, please refer to [28].

Table 3. The L^2 -error and CPU time for Example 4.2.

J	5	6	7	8
L^2 -error	9.598×10^{-06}	3.802×10^{-07}	1.319×10^{-08}	4.198×10^{-10}
Time	0.064	0.93	0.101	0.206
J	9	10	11	12
L^2 -error	1.236×10^{-11}	3.099×10^{-13}	4.227×10^{-14}	1.076×10^{-15}
Time	0.328	0.798	1.012	1.321

Table 4. The comparison between the presented scheme and the finite element method [23] for Example 4.2.

t	Proposed method		[23]	
	$J = 10$	$J = 12$	$h = 1/80$	$h = 1/160$
L^2 -error	3.099×10^{-13}	1.076×10^{-15}	2.652×10^{-09}	6.627×10^{-10}

Table 5. The L^2 -error obtained at different times using 8 and 30 bases for space and time, respectively, (Example 4.2).

t	2	4	6	8	10
L^2 -error	7.150×10^{-24}	1.264×10^{-23}	1.497×10^{-23}	5.078×10^{-23}	3.363×10^{-21}

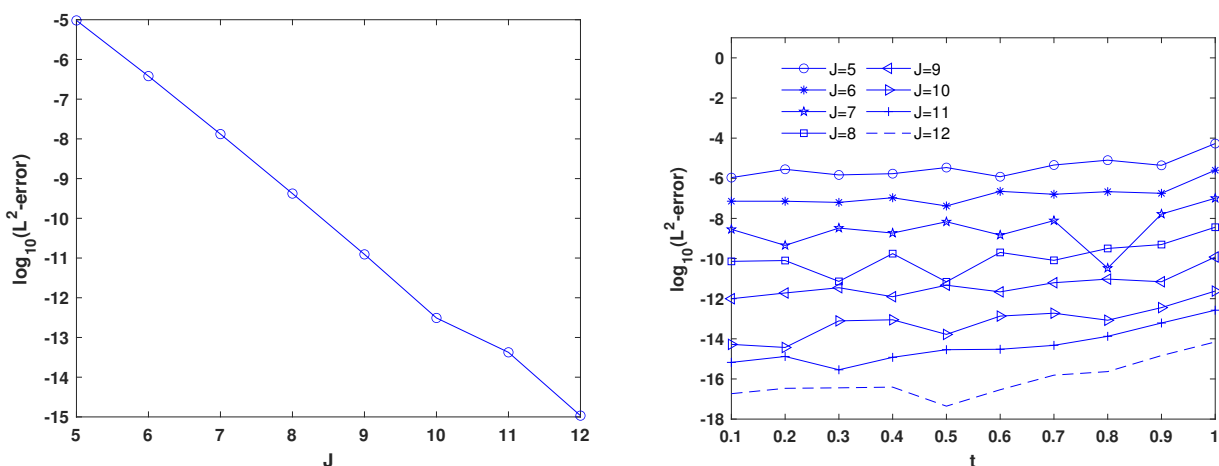


Figure 3. The L^2 -error obtained by different values of J (left) and the L^2 -error obtained by different values of J at different times (right) for Example 4.2.

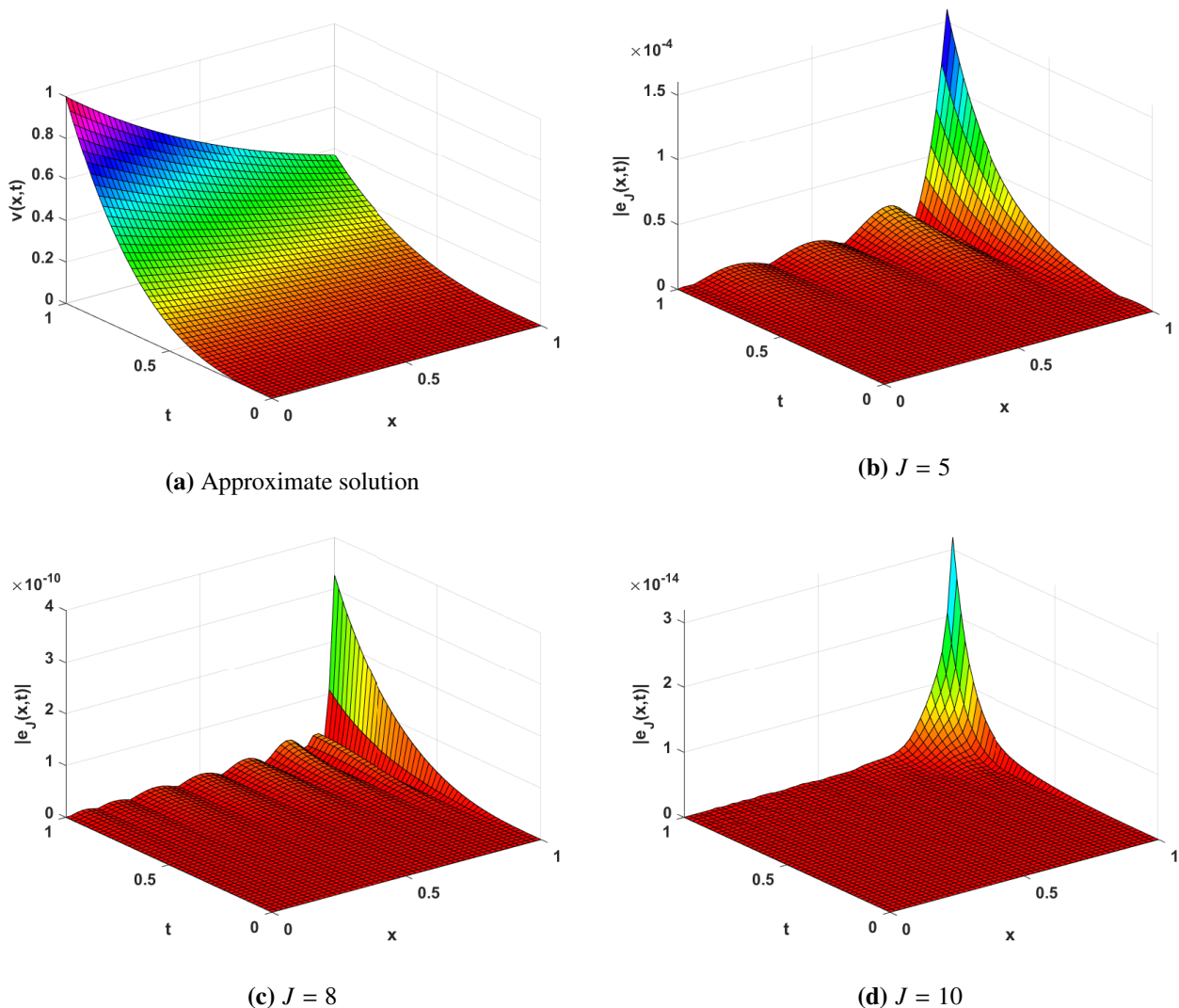


Figure 4. The plot of the approximate solution by choosing $J = 12$ and absolute error with different choices of J for Example 4.2.

Example 4.3. To show the ability of the presented method to solve the two-dimensional fractional diffusion equation, we consider the equation

$$\begin{cases} v_t - \frac{\Gamma(2.2)x^{2.8}y}{6} \frac{\partial^{1.8}v}{\partial x^{1.8}} - \frac{2xy^{2.6}}{\Gamma(4.6)} \frac{\partial^{1.6}v}{\partial x^{1.6}} = -(1 + 2xy)e^{-t}x^3y^{3.6}, & x, y \in [0, 1], \quad t \in (0, T], \\ v|_{t=0} = x^3y^{3.6}, & x, y \in [0, 1], \\ v|_{x=0} = v|_{y=0} = 0, \quad v|_{x=1} = e^{-t}y^{3.6}, \quad v|_{y=1} = e^{-t}x^3, & t \in (0, T]. \end{cases}$$

The exact solution for this equation is $v(x, y, t) = e^{-t}x^3y^{3.6}$ [38].

Table 6 is tabulated to show the convergence of the presented method. As we can see, the error is reduced when the number of bases increases. Also, we reported Table 7 to compare the presented scheme with other methods. To this end, the Kansa method [38] and the finite difference method (FDM) [39] are considered.

Table 6. The L^2 -error for Example 4.3.

$t \setminus J$	5	7	9	11
0.1	9.79×10^{-04}	1.21×10^{-04}	5.24×10^{-05}	1.89×10^{-06}
0.2	1.17×10^{-04}	7.55×10^{-05}	2.65×10^{-05}	2.19×10^{-06}
0.3	1.07×10^{-03}	9.08×10^{-05}	4.32×10^{-05}	3.42×10^{-06}
0.4	1.20×10^{-03}	8.87×10^{-05}	3.63×10^{-05}	3.26×10^{-06}
0.5	4.42×10^{-05}	3.29×10^{-06}	5.46×10^{-06}	9.49×10^{-08}
0.6	1.90×10^{-03}	1.54×10^{-04}	6.39×10^{-05}	4.90×10^{-06}
0.7	2.70×10^{-03}	2.00×10^{-04}	6.81×10^{-05}	8.08×10^{-06}
0.8	3.45×10^{-04}	5.11×10^{-05}	2.11×10^{-05}	8.87×10^{-06}
0.9	1.10×10^{-02}	4.24×10^{-04}	9.92×10^{-05}	9.27×10^{-06}
1.0	3.41×10^{-02}	6.52×10^{-04}	1.07×10^{-04}	4.75×10^{-05}

Table 7. Maximum absolute error at $t = 1$ for Example 4.3.

t	Proposed method $J = 10$	Kansa method [38] $\Delta x = \Delta y = \Delta t = 0.1$	FDM [39] $\Delta x = \Delta y = \Delta t = 0.1$
L^2 -error	1.24×10^{-05}	1.13×10^{-03}	1.26×10^{-03}

Example 4.4. Consider the following SFADE:

$$\begin{cases} v_t + v_x + v - \frac{\partial^\mu v}{\partial x^\mu} = 0, & \mu \in (1, 2], \quad x \in [0, 1], \quad t \in [0, 1], \\ v(x, 0) = \frac{1}{\sqrt{2\pi}} e^{-\frac{x^2}{2}}, & x \in [0, 1], \\ v(0, t) = 0, \quad v(1, t) = 0, & t \in [0, 1]. \end{cases}$$

No exact solution is available for this example. Figure 5, is plotted to demonstrate the approximate solution. To demonstrate the efficiency of the presented schemes for non-integer values of μ , Figure 6 is plotted. Note that

$$\lim_{\mu \rightarrow m} {}^c D_0^\mu v(x, 1) = v^{(m)}(x, 1),$$

$$\lim_{\mu \rightarrow m-1} {}^c D_0^\mu v(x, 1) = v^{(m-1)}(x, 1) - v^{(m-1)}(0, 1).$$

Our results confirm this, and we can verify that when $\mu \rightarrow m$, the estimated solutions with increasing μ tend to the results for m .

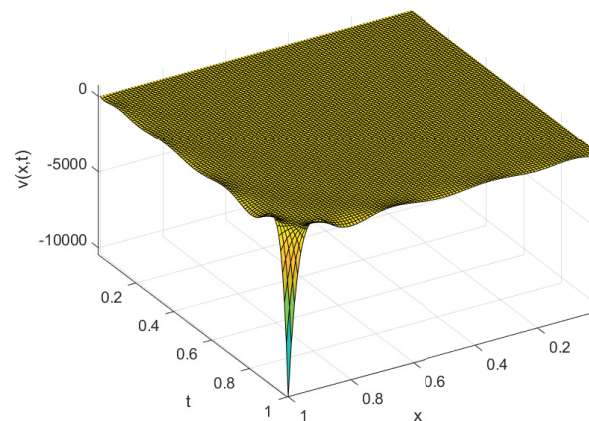


Figure 5. The approximate solution obtained by $J = 10$ for Example 4.4.

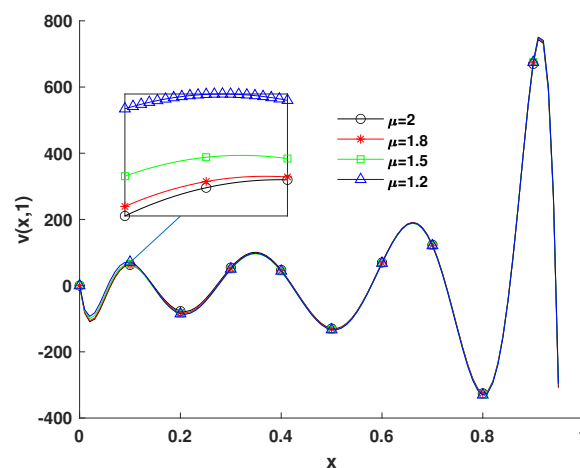


Figure 6. The approximate solution for different choices of μ for Example 4.4.

5. Conclusions

The Galerkin method is a highly effective and efficient technique widely recognized for solving various equations. On the other hand, CCFs are highly effective and powerful bases in numerical techniques due to their inherent properties. Hence, we consider using the Galerkin method based on CCFs to solve the space-fractional advection-diffusion equation. After introducing the CCFs, the Caputo fractional derivative (CFD) is represented based on these bases as an operational matrix. Applying the Galerkin method reduces the desired equation into a system of algebraic equations. Several examples have been solved by the presented method to confirm the convergence analysis presented in Section 3 and to demonstrate the accuracy and ability of the scheme. It is worth noting that the presented method is effective for solving such problems. The method presented here provides accurate solutions and is easier to implement than the finite element method. In addition, using this

method leads to a reduction in computational cost, thanks to the CCFs' properties.

Author contributions

Haifa Bin Jebreen: Conceptualization, Methodology, Software, Validation, Formal analysis, Investigation, Writing—original draft, Writing—review & editing, Funding acquisition; Hongzhou Wang: Formal analysis, Investigation, Software, Validation, Investigation, Writing—original draft, Writing—review & editing. All authors have read and agreed to the published version of the manuscript.

Use of AI tools declaration

The authors declare they have not used Artificial Intelligence (AI) tools in the creation of this article.

Conflict of interest

The authors declare that they have no conflicts of interest.

Funding

This project was supported by Researchers Supporting Project number (RSP2024R210), King Saud University, Riyadh, Saudi Arabia.

References

1. J. Liu, F. Geng, An explanation on four new definitions of fractional operators, *Acta Math. Sci.*, **44** (2024), 1271–1279. <https://doi.org/10.1007/s10473-024-0405-7>
2. M. Arif, F. Ali, I. Khan, K. S. Nisar, A time fractional model with non-singular kernel the generalized couette flow of couple stress nanofluid, *IEEE Access*, **8** (2020), 77378–77395. <https://doi.org/10.1109/ACCESS.2020.2982028>
3. A. Chang, H. Sun, C. Zheng, B. Lu, C. Lu, R. Ma, et al., A time fractional convection-diffusion equation to model gas transport through heterogeneous soil and gas reservoirs, *Physica A*, **502** (2018), 356–369. <https://doi.org/10.1016/j.physa.2018.02.080>
4. J. A. Tenreiro Machado, M. F. Silva, R. S. Barbosa, I. S. Jesus, C. M. Reis, M. G. Marcos, et al., Some applications of fractional calculus in engineering, *Math. Probl. Eng.*, **2010** (2010), 1–34. <https://doi.org/10.1155/2010/639801>
5. F. Mainardi, *Fractional calculus and waves in linear viscoelasticity*, Imperial College Press, 2010. <https://doi.org/10.1142/p614>
6. M. Asadzadeh, B. N. Saray, On a multiwavelet spectral element method for integral equation of a generalized Cauchy problem, *BIT Numer. Math.*, **62** (2022), 1383–1416. <https://doi.org/10.1007/s10543-022-00915-1>

7. A. K. Gupta, S. Saha Ray, Wavelet methods for solving fractional order differential equations, *Math. Probl. Eng.*, **2014** (2014), 140453. <https://doi.org/10.1155/2014/140453>
8. L. Shi, B. N. Saray, F. Soleymani, Sparse wavelet Galerkin method: Application for fractional Pantograph problem, *J. Comput. Appl. Math.*, **451** (2024), 116081. <https://doi.org/10.1016/j.cam.2024.116081>
9. P. Thanh Toan, T. N. Vo, M. Razzaghi, Taylor wavelet method for fractional delay differential equations, *Eng. Comput.*, **37** (2021), 231–240. <https://doi.org/10.1007/s00366-019-00818-w>
10. V. Daftardar-Gejji, A. Jafari, Adomian decomposition: A tool for solving a system of fractional differential equations, *J. Math. Anal. Appl.*, **301** (2005), 508–518. <https://doi.org/10.1016/j.jmaa.2004.07.039>
11. B. Benkerrouche, D. Baleanu, M. S. Soud, A. Hakem, Boundary value problem for nonlinear fractional differential equations of variable order via Kuratowski MNC technique, *Adv. Differ. Equ.*, **2021** (2021), 365. <https://doi.org/10.1186/s13662-021-03520-8>
12. M. Lakestani, M. Dehghan, The use of Chebyshev cardinal functions for the solution of a partial differential equation with an unknown time-dependent coefficient subject to an extra measurement, *J. Comput. Appl. Math.*, **235** (2010), 669–678. <https://doi.org/10.1016/j.cam.2010.06.020>
13. G. J. Fix, J. P. Roop, Least squares finite element solution of a fractional order two-point boundary value problem, *Comput. Math. Appl.*, **48** (2004), 1017–1033. <https://doi.org/10.1016/j.camwa.2004.10.003>
14. S. Maji, S. Natesan, Adaptive-grid technique for the numerical solution of a class of fractional boundary-value-problems, *Comput. Methods Differ. Equ.*, **12** (2010), 338–349. <https://doi.org/10.22034/CMDE.2023.55266.2296>
15. R. Garrappa, On some explicit Adams multistep methods for fractional differential equations, *J. Comput. Appl. Math.*, **229** (2009), 392–399. <https://doi.org/10.1016/j.cam.2008.04.004>
16. Y. L. Zhao, P. Zhu, X. M. Gu, X. Zhao, H. Y. Jian, An implicit integration factor method for a kind of spatial fractional diffusion equations, *J. Phys. Conf. Ser.*, **1324** (2019), 012030. <https://doi.org/10.1088/1742-6596/1324/1/012030>
17. Z. Lin, D. Wang, D. Qi, L. Deng, A Petrov-Galerkin finite element-meshfree formulation for multi-dimensional fractional diffusion equations, *Comput. Mech.*, **66** (2020), 323–350. <https://doi.org/10.1007/s00466-020-01853-x>
18. H. Y. Jian, T. Z. Huang, X. L. Zhao, Y. L. Zhao, A fast second-order accurate difference schemes for time distributed-order and Riesz space fractional diffusion equations, *J. Appl. Anal. Comput.*, **9** (2019), 1359–1392. <https://doi.org/10.11948/2156-907X.20180247>
19. P. Biler, W. A. Woźczynski, Global and exploding solutions for nonlocal quadratic evolution problems, *SIAM J. Appl. Math.*, **59** (1998), 845–869. <https://doi.org/10.1137/S003613999631344>
20. W. Y. Tian, W. Deng, Y. Wu, Polynomial spectral collocation method for space fractional advection-diffusion equation, *Numer. Meth. Partial Differ. Equ.*, **30** (2014), 514–535. <https://doi.org/10.1002/num.21822>
21. R. Metzler, J. Klafter, The random walks guide to anomalous diffusion: A fractional dynamics approach, *Phys. Rep.*, **339** (2000), 1–77. [https://doi.org/10.1016/S0370-1573\(00\)00070-3](https://doi.org/10.1016/S0370-1573(00)00070-3)

22. A. Pablo, F. Quirós, A. Rodríguez, J. L. Vázquez, A fractional porous medium equation, *Adv. Math.*, **226** (2011), 1378–1409. <https://doi.org/10.1016/j.aim.2010.07.017>
23. Y. Zheng, C. Li, Z. Zhao, A note on the finite element method for the space-fractional advection diffusion equation, *Comput. Math. Appl.*, **59** (2010), 1718–1726. <https://doi.org/10.1016/j.camwa.2009.08.071>
24. H. Hejazi, T. Moroney, F. Liu, Stability and convergence of a finite volume method for the space fractional advection-dispersion equation, *J. Comput. Appl. Math.*, **255** (2014), 684–697. <https://doi.org/10.1016/j.cam.2013.06.039>
25. A. Jannelli, M. Ruggieri, M. P. Speciale, Numerical solutions of space-fractional advection-diffusion equations with nonlinear source term, *Appl. Numer. Math.*, **155** (2020), 93–102. <https://doi.org/10.1016/j.apnum.2020.01.016>
26. H. Y. Jian, T. Z. Huang, X. M. Gu, Y. L. Zhao, Compact implicit integration factor method for two-dimensional space-fractional advection-diffusion-reaction equations, *J. Phys. Conf. Ser.*, **1592** (2020), 012048. <https://doi.org/10.1088/1742-6596/1592/1/012048>
27. H. Y. Jian, T. Z. Huang, A. Ostermann, X. M. Gu, Y. L. Zhao, Fast IIF-WENO method on non-uniform meshes for nonlinear space-fractional convection-diffusion-reaction equations, *J. Sci. Comput.*, **89** (2021), 13. <https://doi.org/10.1007/s10915-021-01622-9>
28. J. P. Boyd, *Chebyshev and fourier spectral methods*, Dover Publications, 2001.
29. A. Afarideh, F. D. Saei, M. Lakestani, B. N. Saray, Pseudospectral method for solving fractional Sturm-Liouville problem using Chebyshev cardinal functions, *Phys. Scr.*, **96** (2021), 125267. <https://doi.org/10.1088/1402-4896/ac3c59>
30. A. Afarideh, F. D. Saei, B. N. Saray, Eigenvalue problem with fractional differential operator: Chebyshev cardinal spectral method, *J. Math. Model.*, **11** (2021), 343–355. <https://doi.org/10.22124/JMM.2023.24239.2169>
31. F. Tchier, I. Dassios, F. Tawfiq, L. Ragoub, On the approximate solution of partial integro-differential equations using the pseudospectral method based on Chebyshev cardinal functions, *Mathematics*, **9** (2021), 286. <https://doi.org/10.3390/math9030286>
32. M. Shahriari, B. N. Saray, B. Mohammadalipour, S. Saeidian, Pseudospectral method for solving the fractional one-dimensional Dirac operator using Chebyshev cardinal functions, *Phys. Scr.*, **98** (2023), 055205. <https://doi.org/10.1088/1402-4896/acc7d3>
33. K. Sayevand, H. Arab, An efficient extension of the Chebyshev cardinal functions for differential equations with coordinate derivatives of non-integer order, *Comput. Methods Differ. Equ.*, **6** (2018), 339–352. <https://doi.org/20.1001.1.23453982.2018.6.3.6.5>
34. A. Kilbas, H. M. Srivastava, J. J. Trujillo, *Theory and applications of fractional differential equations*, Amsterdam: Elsevier, 2006.
35. Y. Saad, M. H. Schultz, GMRES: A generalized minimal residual method for solving nonsymmetric linear systems, *SIAM J. Sci. Stat. Comput.*, **7** (1986), 856–869. <https://doi.org/10.1137/090705>
36. G. Dahlquist, A. Björck, *Numerical methods*, Englewood Cliffs: Prentice-Hall, 1974.

37. B. N. Saray, M. Lakestani, M. Dehghan, On the sparse multiscale representation of 2-D Burgers equations by an efficient algorithm based on multiwavelets, *Numer. Math. Partial Differ. Equ.*, **39** (2023), 1938–1961. <https://doi.org/10.1002/num.22795>
38. G. Pang, W. Chen, Z. Fu, Space-fractional advection-dispersion equations by the Kansa method, *J. Comput. Phys.*, **293** (2015), 280–296. <https://doi.org/10.1016/j.jcp.2014.07.020>
39. M. M. Meerschaert, H. P. Scheffler, C. Tadjeran, Finite difference methods for two-dimensional fractional dispersion equation, *J. Comput. Phys.*, **211** (2006), 249–261. <https://doi.org/10.1016/j.jcp.2005.05.017>



AIMS Press

© 2024 the Author(s), licensee AIMS Press. This is an open access article distributed under the terms of the Creative Commons Attribution License (<http://creativecommons.org/licenses/by/4.0>)